

# Hofstadter butterflies of bilayer graphene

Norbert Nemeč and Gianaurelio Cuniberti

*Institute for Theoretical Physics, University of Regensburg, D-93040 Regensburg, Germany*

(Dated: October 19, 2006)

We calculate the electronic spectrum of bilayer graphene in perpendicular magnetic fields non-perturbatively. To accommodate arbitrary displacements between the two layers, we apply a periodic gauge based on singular flux vortices of phase  $2\pi$ . The resulting Hofstadter-like butterfly plots show a reduced symmetry, depending on the relative position of the two layers against each other. The zero-energy Landau-level is split up by varying amounts for non-Bernal stacking. [To be tuned up...](#)

PACS numbers: 73.22.-f, 81.05.Uw, 71.70.Di, 71.15.Dx

After the theoretical prediction of the peculiar electronic properties of graphene in 1947 by Wallace<sup>1</sup> and the subsequent studies of its magnetic spectrum,<sup>2</sup> it took half a century until single layers of graphene could be isolated in experiment<sup>3</sup> and its anomalous quantum hall effect could be measured.<sup>4–7</sup> Shortly afterwards, well defined bilayer structures could also be produced and studied for their electronic structure,<sup>8,9</sup> revealing a high technological potential for electronic switching devices. Theoretical studies of such bilayer structures have pointed towards a highly anomalous behavior of the electronic spectrum in magnetic fields, different from either the regular massive electrons or the special Dirac-type electrons of single layer graphene.<sup>10,11</sup>

In this letter, we use the non-perturbative method introduced 1933 by Peierls<sup>12</sup> for the implementation of a

magnetic field in a tight-binding model and used by Hofstadter in 1976 for the discovery of the fractal spectrum of lattice electrons in a magnetic field.<sup>13</sup> Since its discovery, the so-called ‘‘Hofstadter butterfly’’ has been studied for a variety of different systems.<sup>14–21</sup>

Featuring a large variety of topologies, all these systems have in common, that the atoms inside the unit cell are sitting on discrete coordinates. All closed loops have commensurate area and the network is regular enough that the magnetic phases of all links can be determined individually without the need of a continuously defined gauge field. For a bilayer of graphene, such a direct scheme for implementing a magnetic field is possible only for highly symmetric configuration like the Bernal stacking.<sup>11,22</sup> To handle more general configurations, such as continuous displacements between the layers, it is in general unavoidable to choose a continuously defined gauge that fixes the phase for arbitrarily placed atoms. The difficulty that arises can be seen immediately: For any gauge field that is periodic in two dimensions, the magnetic phase of a closed loop around a single unit cell must cancel out exactly, corresponding to a vanishing total magnetic flux. This means in the reverse: any gauge field that results in a nonzero homogeneous magnetic field will invariably break the periodicity of the underlying system.

A solution is as follows: A *magnetic flux vortex* in  $z$ -direction, located in  $(x_0, y_0)$ , can be defined as<sup>23,24</sup>

$$\mathbf{B}(x, y, z) = \Phi_0 \delta(x - x_0) \delta(y - y_0) \mathbf{e}_z$$

with the flux quantum  $\Phi_0 = \frac{h}{e}$ . Physically, such a vortex is equivalent to a vanishing magnetic field, since it leaves the phase of any possible closed path unchanged modulo  $2\pi$ . One possible gauge field resulting in such a single flux vortex would be:

$$\mathbf{A}(\mathbf{r}) = \frac{\Phi_0 (\mathbf{e}_z \times \mathbf{r})}{2\pi (\mathbf{e}_z \times \mathbf{r})^2}$$

Finding a periodic gauge is now simple: to the homogeneous magnetic field, we add a periodic array of flux vortices with such a density that the average magnetic field is exactly zero. For the resulting field, which is physically equivalent to the original, it is now possible to find a gauge field with the same periodicity as the array of vortices. If the underlying system is periodic and

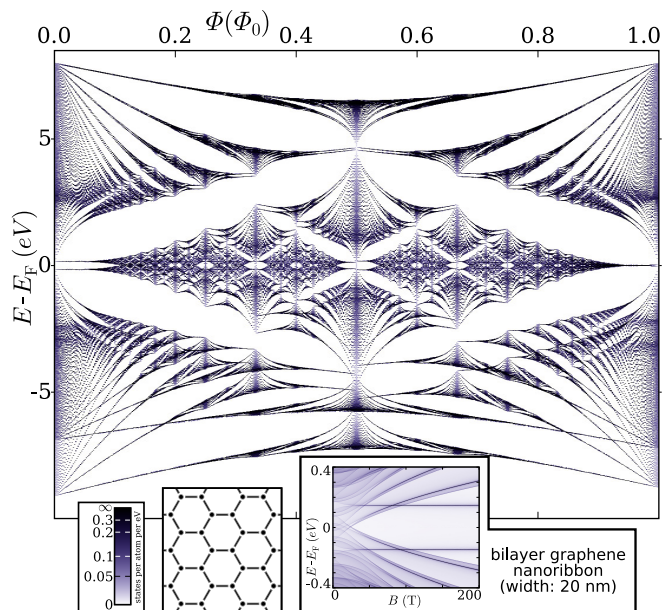


FIG. 1: The Hofstadter butterfly of a bilayer graphene in ‘‘AA-stacking’’ configuration (all atoms are aligned pair-wise on top of each other). The lower right inset shows the density of states of a finite-width ribbon (a pair of (80,0) zigzag-ribbons) in the same configuration at low field near the Fermi energy.

the array of flux vortices has commensurate periodicity, there exists a supercell where the magnetic Hamiltonian is periodic.

One possible periodic gauge that is especially advantageous for numerical implementation is as follows: Consider a two-dimensional periodic system with lattice vectors  $\mathbf{a}_i$  with  $i \in \{x, y\}$ . The reciprocal lattice vectors are  $\tilde{\mathbf{a}}_i$  such that  $\mathbf{a}_i \cdot \tilde{\mathbf{a}}_j = \delta_{ij}$ . The magnetic field is  $\mathbf{B} = \ell\Phi_0(\mathbf{a}_x \times \mathbf{a}_y)$  with  $\ell \in \mathbb{Z}$ . The usual linear—but aperiodic—gauge for this field would be  $\mathbf{A}_{\text{lin}}(\mathbf{r}) = \ell\Phi_0(\mathbf{r} \cdot \tilde{\mathbf{a}}_x)\tilde{\mathbf{a}}_y$ . A periodic gauge can now be defined as:

$$\mathbf{A}(\mathbf{r}) = \ell\Phi_0 \llbracket \mathbf{r} \cdot \tilde{\mathbf{a}}_x \rrbracket (\tilde{\mathbf{a}}_y - \delta \llbracket \mathbf{r} \cdot \tilde{\mathbf{a}}_y \rrbracket \tilde{\mathbf{a}}_x)$$

where  $\llbracket \cdot \rrbracket$  denotes the fractional part of a real number and is defined by

$$\left( \llbracket c \rrbracket \in [0, 1) \wedge c - \llbracket c \rrbracket \in \mathbb{Z} \right) \quad \forall c \in \mathbb{R}.$$

Is  $\wedge$  (the logic “and”) unclear?

To make sure that the phase of every link between two atoms is well-defined in every case, the gauge field is displaced by an infinitesimal amount such that every atom sits either left or right of the divergent line.

The Hamiltonian without magnetic field is based on a tight-binding parametrization originally used for multi-walled carbon nanotubes.<sup>25</sup> It consists of a contribution for nearest neighbors within a layer  $\langle i, j \rangle$  and one for pairs of atoms located on different sheets  $[i, j]$ :

$$\mathcal{H} = -\gamma_0 \sum_{\langle i, j \rangle} c_i^\dagger c_j + \sum_{[i, j]} \gamma_{[i, j]} c_i^\dagger c_j$$

The intralayer hopping parameter is fixed to  $\gamma_0 = 2.66$  eV. The interlayer hopping depends on the distance only:

$$\gamma_{[i, j]} = \frac{\gamma_0}{8} \exp\left(\frac{|\mathbf{r}_i - \mathbf{r}_j| - a}{\delta}\right)$$

with  $a = 3.34$  Å and  $\delta = 0.45$  Å. A cutoff is chosen as  $r_{\text{cutoff}} = a + 5\delta$ . Following the Peierls substitution,<sup>12</sup> the magnetic field  $\mathbf{B}$  is now implemented by multiplying a magnetic phase factor to each link between two atoms  $i$  and  $j$ :

$$\gamma_{i, j}(\mathbf{B}) = \gamma_{i, j}^0 \exp\left(i \frac{2\pi}{\Phi_0} \int_{\mathbf{r}_i}^{\mathbf{r}_j} \mathbf{A}_B(\mathbf{r}) \cdot d\mathbf{r}\right)$$

where the integral is computed on a straight line between the atomic positions  $\mathbf{r}_i$  and  $\mathbf{r}_j$ .

For the bilayer graphene, we arrive thus at a periodic Hamiltonian with a two-dimensional unit-cell containing four atoms and spanning the area of one hexagonal graphene plaquette:  $A_{\text{plaquette}} = \frac{3\sqrt{3}}{2}d_{\text{CC}}^2$ , where  $d_{\text{CC}} = 1.42$  Å is the distance between neighboring carbon atoms. A perpendicular magnetic field, measured in flux per plaquette  $\Phi = A_{\text{plaquette}}B$ , can be applied for

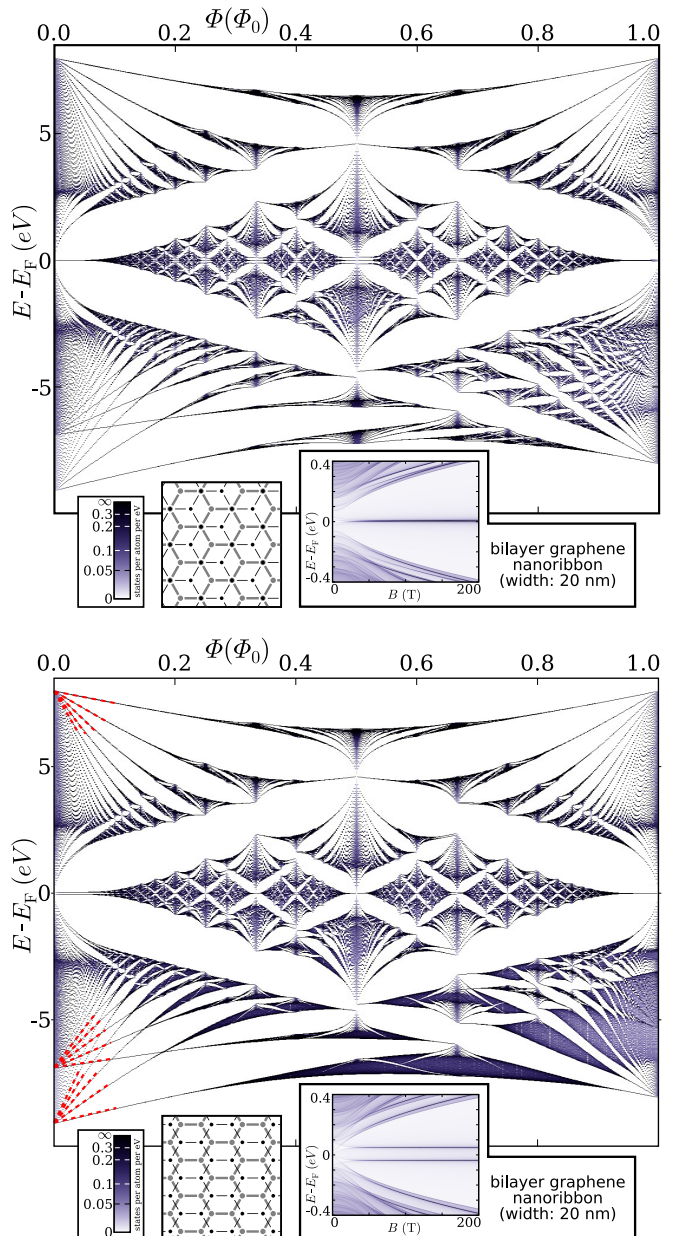


FIG. 2: The Hofstadter butterfly of a bilayer graphene in two differently shifted configurations. Top panel: “Bernal stacking” (also called “AB-stacking”). Bottom panel: an intermediate position between AA- and AB-stacking. In both panels, the inset at the lower right shows the density of states of a corresponding finite-width ribbon. The straight lines overlaid at the energy min- and maximum in the bottom panel are the regular Landau-levels of the massive bands. Near  $E_F$ , one can make out the parabolic traces of the relativistic Landau levels (see text).

commensurate values  $\Phi = (p/q)\Phi_0$  ( $p, q \in \mathbb{Z}$ ) by constructing a supercell of  $q$  unitcells. The corresponding Bloch Hamiltonian  $\mathcal{H}(\mathbf{k})$  is a  $4q \times 4q$  matrix that can be diagonalized numerically for arbitrary values of  $\mathbf{k}$  in the two-dimensional Brillouin zone of area  $4\pi^2/qA_{\text{plaquette}}$ .

To obtain the butterfly plots as displayed in Figs. 1 and 2, we chose  $q = 512$  and  $p = 0, 1, \dots, 512$ , reducing the fraction  $p/q$  to save computation time. For each value of  $\Phi$ , the Brillouin zone, the density of states was calculated from a histogram over the spectral values for a random sampling of  $\mathbf{k}$  over the Brillouin zone. The number of sampling points was chosen individually for different values of  $p$  to achieve convergence of the visual appearance.

In Figs. 1 and 2, the Hofstadter spectra of three differently aligned graphene bilayers are presented. The Bernal stacking (Fig. 2) stands out, as it is the configuration of layers in natural graphite.<sup>22</sup> The other two alignments can be thought of as either mechanically shifted samples or sections of curved bilayers (e.g. sections of large double-wall carbon nanotubes) where the alignment unavoidably varies over distance. Compared to the butterfly of a single sheet of graphene,<sup>15</sup> two asymmetries are visible in all three plots:

The electron-hole symmetry ( $E \leftrightarrow -E$ ) is broken up by the interlayer coupling already at zero magnetic field: while the lowest energy states of a single graphene layer have constant phase over all atoms and can couple efficiently into symmetric and antisymmetric hybrid states of the bilayer system, the states at high energies have alternating phase for neighboring atoms, so interlayer hybridization is prohibited by the second-nearest-neighbor interlayer coupling. For low magnetic fields, two sets of Landau levels can therefore be observed at the bottom of the spectrum, indicating a split of the massive band at the Gamma point into two bands at different energy and with different effective mass (see straight lines overlaid in the bottom panel of Fig. 2). At the top of the spectrum, where the split is prohibited, only one degenerate set of Landau levels appears.

The original periodic symmetry along the  $B$ -field axis at one flux quantum per graphene plaquette is broken up due to the smaller areas formed by interlayer loops. The breaking of this symmetry is comparably small in the AA-stacking configuration (Fig. 1) where loops of the full plaquette area are dominant. In the two configurations displayed in Fig. 2, smaller loops are more important, so the periodicity is perturbed more severely. In the intermediate configuration (Fig. 2, bottom) the fractal patterns are slightly smeared out for high magnetic fields due to the reduced symmetry of the system.

The inset at the lower left corner of all three Hofstadter spectra displays the spectrum of a  $(80,0)@(80,0)$  bilayer graphene ribbon in corresponding configuration, obtained by a method described before<sup>21</sup> that allows handling of continuous magnetic fields. For low magnetic fields, these spectra are strongly influenced by finite size effects. Only for magnetic fields larger than  $B^* \approx 4\Phi_0/d^2$ , which, for a ribbon of width  $d = 20$  nm, relates to  $\sim 60$  T, the spectra of two-dimensional bilayer graphene begin to emerge. Prominent in all three insets are the dark, horizontal pairs of lines at the center, the supersymmetric Landau levels (SuSyLL, see below).

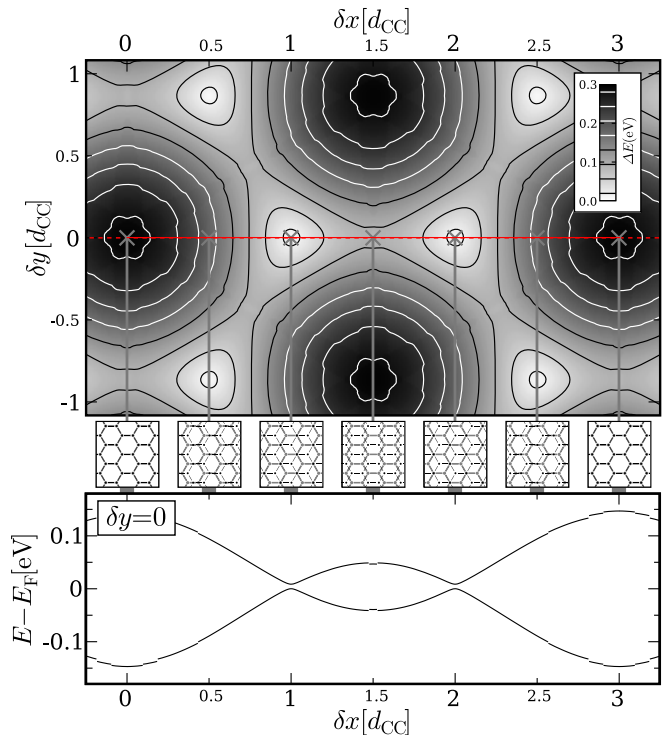


FIG. 3: The evolution of the split of the anomalous Landau level with continuously varying displacement between the two graphene layers. Top panel: The magnitude of the split for displacements in two directions. The dark spots correspond to Bernal stacking where the level is near-degenerate. Bottom panel: the same data along a cut of at  $\delta y = 0$ . The small remaining split at the Bernal stacking configurations originates in the long-range interlayer hoppings contained in the parametrization. The small discontinuities are caused by the cutoff  $r_{\text{cut}}$ .

While these represent discrete levels in two-dimensional graphene sheets, they are broadened by the finite width of the ribbon to a peak of the same shape as in carbon nanotubes.<sup>21,26</sup> The dependence of peak on the width  $W$  of the ribbon is captured by the functional form of the density of states per atom  $\rho_{\text{DOS}}$ :

$$\rho_{\text{DOS}}(E, B, W) = f((E - E_0)W, BW^2)$$

where  $E_0$  is the position of the maximum.

Single layer graphene is known to feature an anomalous supersymmetric Landau level (SuSyLL) at the Fermi energy.<sup>2,4,27</sup> Neglecting Zeeman-splitting, this level is twice spin-degenerate and half-filled. For bilayer graphene in Bernal stacking (Fig. 2 top), the SuSyLL of the two layers have been shown to be protected by symmetry and to remain (fourfold) degenerate.<sup>11</sup> In Fig. 1, this degeneracy can be observed to be lifted for displaced bilayers, leading to a split of the SuSyLL into a bonding and an antibonding hybrid state in the two layers, each twice spin-degenerate. The continuous evolution of the split for varying displacement of the two layers against each other is displayed in Fig. 3. The split

reaches its maximum of  $\Delta E \sim 0.3$  eV for AA-stacking configuration and is minimal for Bernal stacking. For simpler tight-binding parametrizations that take into account only first and second nearest neighbor interlayer hoppings, the degeneracy in the Bernal configuration is known to be exact.<sup>11</sup> Here, in contrast to these previous findings, this degeneracy is split up by  $\Delta E \sim 0.01$  eV due to interlayer hoppings of a longer range.

To conclude: We have used a method that allows the implementation of a magnetic field in periodic systems with arbitrarily positioned atoms. A tight-binding parametrization for graphite interlayer interactions with arbitrary displacements was then used to calculate the Hofstadter spectrum of bilayer graphene in three characteristic configurations, revealing common features like the electron-hole symmetry breaking and differences, especially in the breaking of the  $B$ -field periodicity. A close look at the supersymmetric Landau level at low fields near the Fermi energy revealed a breaking of the previously found symmetry, resulting in a split of the level, de-

pending on the lateral displacement of the two graphene layers against each other.

**ToDo:**

- Go through the pile of papers that should perhaps be cited?

**Check list**

- before submitting, we should remember to send a copy for comments to

1. ...

We acknowledge fruitful discussions with Inanc Adagideli. **Others?**

This work was funded by the Volkswagen Foundation under grant No. I/78 340 and by the European Union grant CARDEQ under contract No. IST-021285-2. Support from the Vielberth Foundation is also gratefully acknowledged. **Are all of these actually involved?**

- 
- <sup>1</sup> P. R. Wallace, Phys. Rev. **71**, 622 (1947).  
<sup>2</sup> J. W. McClure, Phys. Rev. **104**, 666 (1956).  
<sup>3</sup> K. S. Novoselov, D. Jiang, F. Schedin, T. J. Booth, V. V. Khotkevich, S. V. Morozov, and A. K. Geim, Proc. Natl. Acad. Sci. USA **102**, 10451 (2005).  
<sup>4</sup> V. Gusynin and S. Sharapov, Phys. Rev. Lett. **95**, 146801 (2005).  
<sup>5</sup> Y. Zhang, Y.-W. Tan, H. L. Stormer, and P. Kim, Nature **438**, 201 (2005).  
<sup>6</sup> K. S. Novoselov, A. K. Geim, S. V. Morozov, D. Jiang, M. I. Katsnelson, I. V. Grigorieva, S. V. Dubonos, and A. A. Firsov, Nature **438**, 197 (2005).  
<sup>7</sup> Y. Zhang, Z. Jiang, J. P. Small, M. S. Purewal, Y.-W. Tan, M. Fazlollahi, J. D. Chudow, J. A. Jaszczak, H. L. Stormer, and P. Kim, Phys. Rev. Lett. **96**, 136806 (2006).  
<sup>8</sup> T. Ohta, A. Bostwick, T. Seyller, K. Horn, and E. Rotenberg, Science **313**, 951 (2006).  
<sup>9</sup> D. Graf, F. Molitor, K. Ensslin, C. Stampfer, A. Jungen, C. Hierold, and L. Wirtz cond-mat/0607562 (unpublished).  
<sup>10</sup> K. S. Novoselov, E. McCann, S. V. Morozov, V. I. Fal'ko, M. I. Katsnelson, U. Zeitler, D. Jiang, F. Schedin, and A. K. Geim, Nature Physics **2**, 177 (2006).  
<sup>11</sup> E. McCann and V. I. Fal'ko, Phys. Rev. Lett. **96**, 086805 (2006).  
<sup>12</sup> R. Peierls, Z. Phys. **80**, 763 (1933).  
<sup>13</sup> D. R. Hofstadter, Phys. Rev. B **14**, 2239 (1976).  
<sup>14</sup> F. H. Claro and G. H. Wannier, Phys. Rev. B **19**, 6068 (1979).  
<sup>15</sup> C. Krefl and R. Seiler, J. Math. Phys. **37**, 5207 (1996).  
<sup>16</sup> C. Albrecht, J. H. Smet, K. von Klitzing, D. Weiss, V. Umansky, and H. Schweizer, Phys. Rev. Lett. **86**, 147 (2001).  
<sup>17</sup> D. Osadchy and J. E. Avron, J. Math. Phys. **42**, 5665 (2001).  
<sup>18</sup> Y. Iye, E. Kuramochi, M. Hara, A. Endo, and S. Katsumoto, Phys. Rev. B **70**, 144524 (2004).  
<sup>19</sup> J. G. Analytis, S. J. Blundell, and A. Ardavan, Am. J. Phys. **72**, 613 (2004).  
<sup>20</sup> L. Jiang and J. Ye, cond-mat/0601083 (unpublished).  
<sup>21</sup> N. Nemeč and G. Cuniberti, Phys. Rev. B, to appear (2006), cond-mat/0607096.  
<sup>22</sup> J. D. Bernal, Proc. Phys. Soc. London, Sect. A **106**, 749 (1924).  
<sup>23</sup> A. Trellakis, Phys. Rev. Lett. **91**, 056405 (2003).  
<sup>24</sup> W. Cai and G. Galli, Phys. Rev. Lett. **92**, 186402 (2004).  
<sup>25</sup> S. Roche, F. Triozon, A. Rubio, and D. Mayou, Phys. Rev. B **64**, 121401(R) (2001).  
<sup>26</sup> H.-W. Lee and D. S. Novikov, Phys. Rev. B **68**, 155402 (2003).  
<sup>27</sup> M. Ezawa (2006), unpublished, cond-mat/0606084.